

STRUCTURE OF FEROXYHITE AS DETERMINED BY SIMULATION OF X-RAY DIFFRACTION CURVES

V. A. DRITS, B. A. SAKHAROV AND A. MANCEAU*

Geological Institute of the Russian Academy of Science, 7 Pyzhevsky prospekt, 109017 Moscow, Russia and

** LGIT-IRIGM, Université Joseph Fourier and CNRS, BP53X, 38041 Grenoble, France*

(Received 12 May 1992; revised 3 November 1992)

ABSTRACT: Powder X-ray diffraction (XRD) curves were calculated for the different structural models so far proposed for ferroxihite (δFeOOH). The influence on XRD features of different structural parameters, including site occupancy of Fe atoms, atomic coordinates, content and distribution of stacking faults, and dimension of coherent scattering domains, were considered. On the basis of agreement between experimental and simulated curves it is shown that δFeOOH is a mixture of ferroxihite proper and ultradispersed hematite in the 9:1 volume ratio. Ferroxihite proper consists of hexagonal close packing of anions containing 5% stacking faults. Iron atoms occupy only octahedral sites and are distributed in such a way that face-sharing filled octahedral pairs regularly alternate with vacant octahedral pairs along the *c* axis. This distribution of Fe atoms is quite similar to that established by Patrat *et al.* (1983), but in each pair, Fe atoms are displaced by the same value of 0.3 Å in opposite directions away from the centre of their octahedron. Nearest Fe–Fe distances calculated for the model proposed (2.88, 3.01, 3.39 and 3.73 Å) practically coincide with those found by EXAFS spectroscopy for the same sample (2.91, 3.04, 3.41 and 3.7–3.8 Å).

Among Fe oxyhydroxide polymorphs, δFeOOH has been the least studied. It can be easily synthesized under laboratory conditions, and it is generally characterized by high dispersion, relatively poor crystallinity and low stability (Glemser & Gwinner, 1939; Dasgupta, 1961; Feitknecht *et al.*, 1969; Misawa *et al.*, 1970; Chukhrov *et al.*, 1976; Povitskii *et al.*, 1976; Carlson & Schwertmann, 1980). Chukhrov *et al.* (1973, 1976) found this δ polymorph among Fe hydroxides of soils and oceanic Fe–Mn formations and called it ferroxihite (Fx). To distinguish the natural phase from the synthetic one, the former was labelled $\delta'\text{FeOOH}$ (Chukhrov *et al.*, 1973). More recently, a second continental occurrence was reported in rusty precipitates from Finland (Carlson & Schwertmann, 1980).

Francombe & Rooksby (1959) were the first to suggest a structural model for δFeOOH having a hexagonal unit-cell with $a = 2.95$ Å and $c = 4.53$ Å. In terms of their model, the anions form a hexagonal packing in which 40% of octahedral and 5% of tetrahedral sites available are occupied statistically by Fe^{3+} . They supposed that the presence of cations in tetrahedral sites would explain the ferromagnetic properties of δFeOOH on the basis of a mechanism similar to that operative in $\gamma\text{Fe}_2\text{O}_3$. The same site occupancy of Fe^{3+} was also assumed by Bernal *et al.* (1959), Dasgupta (1961) and Chukhrov *et al.* (1976). Okamoto (1968) calculated X-ray reflection intensities for several structural models of δFeOOH varying in their Fe^{3+} distributions over octahedral and tetrahedral sites. On a qualitative basis, his results tended to support the idea that Fe occurs exclusively in octahedral sites.

Confirmation by XRD of the existence of face-sharing octahedra was not conclusive overall, but Okamoto (1968) supposed that the octahedra are not face-sharing on the basis of magnetic properties. More precise data concerning the Fe^{3+} distribution over octahedral and tetrahedral sites in δFeOOH were obtained using neutron diffraction by Pernet *et al.* (1984) who concluded that the tetrahedra are not filled. In addition, Pernet *et al.* (1984) inferred that the crystallographic structure of δFeOOH consists of an antiferromagnetic coupling of Fe^{3+} ions in face-sharing octahedra. Lastly, local ordering in the distribution of vacant and occupied octahedral Fe sites was recognized by Patrat *et al.* (1983). In terms of their model, face-sharing octahedral pairs occupied by Fe atoms regularly alternate along [001] with vacant octahedral pairs. Certain limitations were also imposed on the possible Fe–Fe and Fe– \diamond distances, where \diamond represents vacant octahedra.

Chukhrov *et al.* (1976) described two varieties of δFeOOH differing in their hexagonal unit-cell parameters. One had the same values as those previously described in literature for natural and synthetic species ($a = 2.93 \text{ \AA}$, $c = 4.6 \text{ \AA}$), but the second was characterized by $a = 5.08 \text{ \AA}$ and $c = 4.6 \text{ \AA}$. To explain the a value, these authors suggested that δFeOOH possesses a two-layer periodicity along c in which each of two layers differ in content and distribution pattern of Fe atoms. In the idealized case, one layer contains Fe atoms distributed according to the hematite pattern (two occupied octahedra regularly alternating with a vacant one along $[\bar{1}10]$: Fe–Fe– \diamond –Fe...), while in the second, Fe atoms are distributed according to an anti-hematite pattern (two vacant octahedra alternating with an occupied one: \diamond – \diamond –Fe– \diamond ...). The authors admitted that some of the Fe atoms may “move” from the hematite layer to the anti-hematite one, leading, in the limit, to a disordered Fe distribution, i.e. to a phase with $a = 2.96 \text{ \AA}$. The distribution pattern of Fe proposed by Okamoto (1968) and Chukhrov *et al.* (1976) is radically different from that of the Patrat’s model (1983). The former model maximizes the number of edge- and corner-sharing octahedra over that of face-sharing ones (ideally, the number of face-sharing should be 0). In contrast, the number of face linkages is at a maximum in Patrat’s model (each Fe octahedron shares a face).

This overview of the literature indicates that some peculiarities of the δFeOOH structure are not well understood. All the previous works assume, *a priori*, that feroxyhite has an idealized hexagonal anionic packing. One may suppose, however, that the structure contains a certain number of stacking faults. In addition, some of the details in the δFeOOH local structure seem unreasonable in terms of crystal chemistry. Specifically, in Patrat’s (1983) model, 50% of Fe–(O,OH) interatomic distances are abnormally short (1.75 \AA) or long (2.35 \AA).

This work aims at determining precisely the real local and average structure of feroxyhite. The approach used for determining the average structure consisted of calculating the distribution of intensities of XRD reflections for various structural models, and then comparing these intensities to those of the experimental powder XRD curves. Parameters which have been varied include: site occupancies; atomic coordinates; type, content, and distribution of stacking faults; and dimensions of coherent scattering domains (CSD). Methodological and theoretical aspects of this approach have been described by Plançon (1981), Sakharov *et al.* (1982a,b) and Drits & Tchoubar (1990) who showed, with the help of examples, how this approach can be effective in describing the actual defect structure of microdivided minerals. The local structure of the same sample of feroxyhite has been previously studied by EXAFS spectroscopy (Manceau & Drits, 1993), and the final section of the paper will compare the present XRD results with the EXAFS work.

MATERIALS AND EXPERIMENTAL RESULTS

The δFeOOH sample was synthesized according to the procedure described by Carlson & Schwertmann (1980). The XRD pattern was obtained with a DRON-UM-1 automatic powder diffractometer with a horizontal goniometer, a vertical sample holder, and a graphite monochromator using $\text{Cu-K}\alpha$ radiation. The diffractometer was equipped with a set of narrow vertical slits (0.1–0.25 mm) to limit the horizontal beam divergence, and Sollers slits with an angular aperture of 0.5° to limit the vertical beam divergence. Intensities were measured every $0.05^\circ 2\theta$ with a counting time of 100 s per point. In order to estimate the background, the XRD pattern of a hematite sample was also recorded under the same conditions.

The XRD pattern for feroxyhite contains four reflections at 2.55, 2.23, 1.70 and 1.47 Å (Fig. 1). Analysis of their positions led to a hexagonal cell with $a = 2.947 \pm 0.002$ Å and $c = 4.56 \pm 0.01$ Å. The different reflections of feroxyhite do not have the same width, and the background intensity increases between 28 and $42^\circ 2\theta$. This diffuse maximum is not an instrumental artefact because the background intensity for the standard hematite sample was practically constant over the 24 – $70^\circ 2\theta$ range. Furthermore, a similar phenomenon has been repeatedly observed by several others (e.g. Carlson & Schwertmann, 1980; Koch *et al.*, 1987).

SIMULATION OF XRD CURVES

This section presents and discusses XRD curves simulated for the different structural models. Effects of site occupancies, atomic positions, stacking faults, coherent scattering domain (CSD) dimensions, and Debye-Scherrer B factor on the distribution of intensity of X-ray reflections will be considered.

The Francombe & Rooksby (1959) model

As mentioned in the introduction, atoms in this model are distributed according to the hexagonal pattern $\text{Ab}_1\text{c}_1\text{a}_1\text{Ba}_2\text{c}_2\text{b}_2\text{A}\dots$, where A and B stand for O and OH positions of the

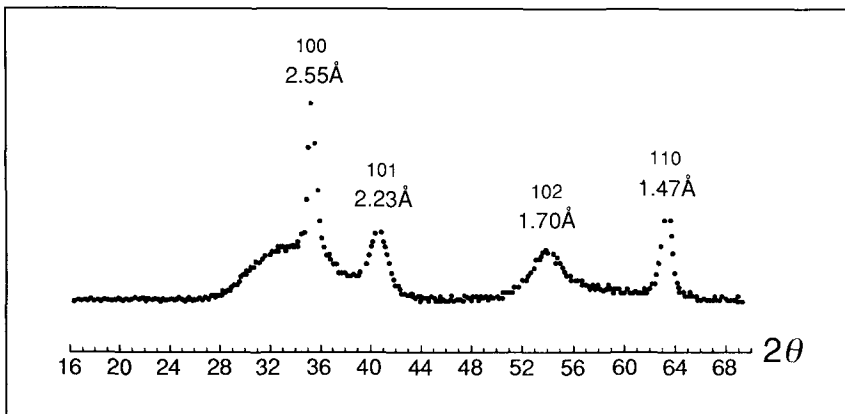


Fig. 1. Experimental XRD curve for feroxyhite. $\text{Cu-K}\alpha$ radiation.

hexagonal close packing, a and b denote centres of tetrahedra, and c , centres of octahedra. Fractional x , y and z coordinates are reported in Table 1 (space group $P\bar{3}m1$). Unit-cell parameters used in the calculation were $a = 2.95 \text{ \AA}$ and $c = 4.56 \text{ \AA}$. The CSDs were modelled as discs, 110 \AA in diameter in the ab plane. Discs 4, 5, 6 and 7 unit-cells thick occurred with equal probability (average thickness $\bar{H} = 25 \text{ \AA}$). The choice of CSD diameter was determined by the shape and intensity ratio of 100 and 110 reflections which have been found to be identical in both the experimental and simulated XRD curves. For this reason, this value of CSD diameter has also been used in all the models considered hereafter. Iron was assumed to occupy 40% and 5% of available octahedral and tetrahedral sites, respectively. The XRD curve simulated for this model is shown in Fig. 2a. It differs substantially from the experimental one in intensity ratios for $10l$ reflections.

The Okamoto (1968) model

Calculations were performed keeping the same anionic packing, cell constants, and CSD dimensions ($\bar{H} = 25 \text{ \AA}$) as in the previous model; however, Fe atoms are only 6-fold coordinated in this model, and the occupancy of available octahedral sites is 50%. Qualitatively, the calculated curve (Fig. 3a) differs from the experimental one (Fig. 1) in the intensity ratio of the 101 and 102 reflections: for the simulated curve, $I(101) < I(102)$ whereas the experimental one shows the reverse relationship. Comparison of Fig. 3a and Fig. 3b illustrates the dependence of $hk0$ and $h0l$ reflection intensities on the CSD average thickness. As expected, for a fixed disc diameter, an increase in the CSD thickness leads to an increase in $h0l$ reflection intensities compared to the $hk0$ intensity, and to a decrease in the $I(101)/I(102)$ ratio and peak widths. No variation in CSD dimensions, however, produces a satisfactory agreement between the simulated and experimental XRD curves.

The Okamoto (1968) model containing stacking faults

The feroxyhite structure in this model contains defects in the anionic hexagonal close packing (hcp) resulting from intrusions of cubic close-packing (ccp) fragments. Six layer types were used to construct this model: 1: AbC; 2: AcB; 3: BaC; 4, BcA; 5: CaB; and 6: CbA, where letters A, B and C denote the O and OH positions, and a , b , c stand for the octahedral cation sites. Each of the six layers was described by a hexagonal unit-cell with

TABLE 1. Atomic coordinates of atoms in hexagonal close-packing.

	x	y	z
A	0	0	0
B	1/3	2/3	0.5
a_1	0	0	0.125
a_2	0	0	0.375
b_1	1/3	2/3	0.625
b_2	1/3	2/3	0.875
c_1	2/3	1/3	0.25
c_2	2/3	1/3	0.75

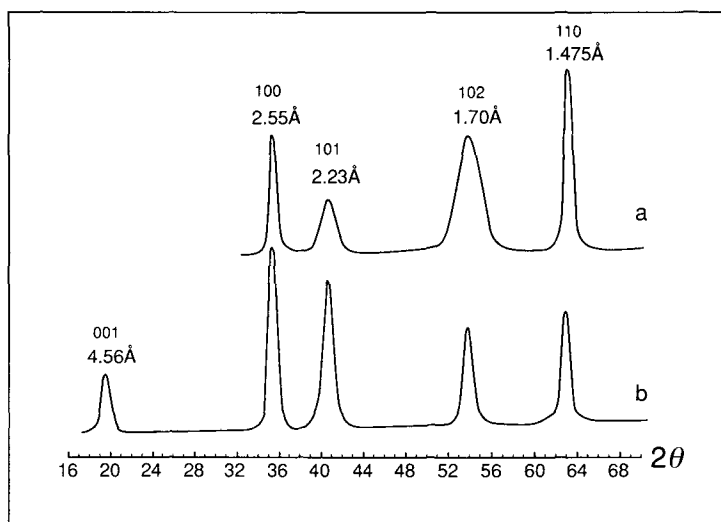


FIG. 2. XRD curves calculated for: (a) The Francombe & Rooksby (1959) model; CSD containing 4, 5, 6 and 7 unit-cells occur with equal probability. $\bar{H} = 25 \text{ \AA}$; (b) the Patrat *et al.* (1983) model; CSD containing 10, 11, 12 ... 20 unit-cells are distributed with equal probability. $\bar{H} = 68 \text{ \AA}$. Cu- $K\alpha$ radiation.

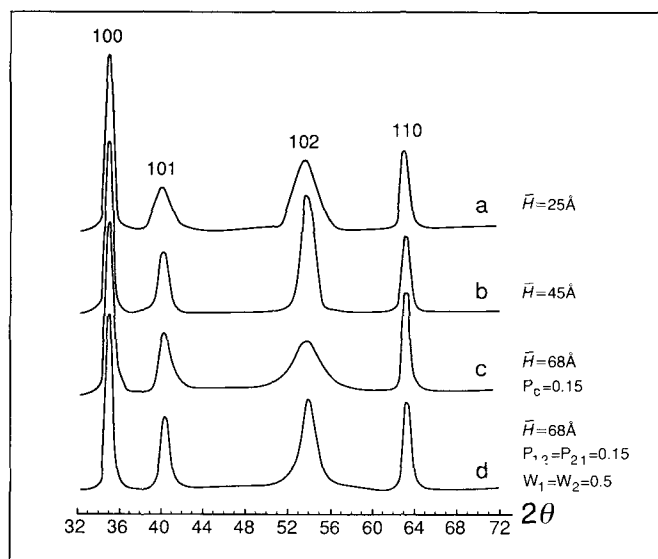


FIG. 3. XRD curves calculated for: (a) the Okamoto (1968) model containing disc-shaped CSD, 110 \AA in diameter and 25 \AA in thickness (\bar{H}). Discs containing 4, 5, 6 and 7 unit-cells occur with equal probability; (b) the same model containing disc-shaped CSD, 110 \AA in diameter and 45 \AA in average thickness. Discs containing 7, 8, 9 ... 12 unit-cells occur with equal probability; (c) the six-component defective structure in which 15% ccp fragments are randomly distributed within the hcp matrix. CSD containing 12, 13, 14 ... 17 unit-cells occur with equal probability. $\bar{H} = 68 \text{ \AA}$; (d) the two-component defective structure with $W_1 = W_2$ and $P_{12} = P_{21} = 0.15$. CSD containing 12, 13, 14 ... 17 unit-cells occur with equal probability. $\bar{H} = 68 \text{ \AA}$. Cu- $K\alpha$ radiation.

$a = 2.947 \text{ \AA}$ and $c = 2.28 \text{ \AA}$. The fractional z -coordinates were 0, 0.5 and 1.0 for the lower anion, the octahedral cation and the upper anion, respectively. The number of anions and cations per A, B, C, a, b, c position in the unit-cell was 0.5. Various layer types occurred with equal probabilities ($W_i = 1/6$), and layer-type combinations were possible only under the condition that a layer terminating with anions having a given set of x, y coordinates was followed by a layer beginning with anions having the same x, y coordinates. For example, an AcB layer could be followed only by BaC or BcA to form fragments of cubic (AcBaC) or hexagonal (AcBcA) close packings, respectively. Sequences of various layer types may describe any intermediate pattern in the alternation of hcp and ccp fragments from the idealized hexagonal packing of the idealized cubic one. The occurrence probabilities for various sequences can be easily calculated if conjunction probabilities, P_{ij} ($i, j = 1, 2, \dots, 6$, $\sum_j P_{ij} = 1$), are included describing the probability for layer j to follow layer i . These coefficients are conveniently presented as a matrix

i/j	1	2	3	4	5	6
1	0	0	0	0	P_{15}	P_{16}
2	0	0	P_{23}	P_{24}	0	0
3	0	0	0	0	P_{35}	P_{36}
4	P_{41}	P_{42}	0	0	0	0
5	0	0	P_{53}	P_{54}	0	0
6	P_{61}	P_{62}	0	0	0	0

The value of P_{ij} for a given set of i and j is at the intersection of the row i and column j . For example, P_{42} defines the probability for layer AcB (No. 2) to follow layer BcA (No. 4). The product $W_4 P_{42}$ determines the complete occurrence probability for the BcAcB layer sequence along the c axis. Thus, the occurrence probability is calculated for any layer sequence with the given distribution of layer types. For $P_{16} = P_{24} = P_{35} = P_{42} = P_{53} = P_{61} = P_h$ and $P_{15} = P_{23} = P_{36} = P_{41} = P_{54} = P_{62} = P_c$, various P_h/P_c ratios define defective structures differing in relative contents of hcp and ccp fragments. For example, the ABABCb anionic sequence corresponds to the layer-type sequence 24235, and its occurrence probability is $W_2 P_{24} P_{42} P_{23} P_{35} = 1/6 P_h^3 P_c$.

In terms of this model, for $P_c = 0.15$, i.e. for 15% ccp fragments distributed within the hcp matrix, the XRD curve simulated for $\bar{H} = 68 \text{ \AA}$ shows considerable broadening of the 102 reflection compared to its width in the absence of stacking faults (compare Fig. 3b and 3c).

There is another way to introduce stacking faults into anionic hcp: two structural layer fragments AcBcA (number 1) and AbCbA (number 2) were assumed to have an irregular distribution within the same crystal leading to the formation of defective structures. Each of these fragments was described by the same unit-cell parameters ($a = 2.95 \text{ \AA}$ and $c = 4.58 \text{ \AA}$). The number of anions per A position in the unit-cell of these fragments was 0.5. Two different models were considered. In the first, both fragments occur with the same probability ($W_1 = W_2 = 0.5$) while the pattern in their distribution is controlled by the parameter P_{ij} ($i, j = 1, 2$). The value of this parameter defines the probability for fragment j to follow fragment i . This value was varied from 0 (pure hcp) to 0.5 (random alternation of the fragments in question). In the second model the numbers of fragments 1 and 2 were different ($W_1 \neq W_2$), and these fragments alternated completely at random. As the XRD curves calculated for these two models have, in general, the same diffraction features as for the 6-component model described above, the results are not shown.

The presence of stacking faults is not always easy to recognize by a visual observation of

XRD patterns in the case of thick CSD. For instance, the XRD curve shown in Fig. 3d was calculated for a 2-component defective model with $\bar{H} = 68 \text{ \AA}$, $W_1 = W_2 = 0.5$ and $P_{12} = P_{21} = 0.15$. The widths of the reflections are similar to those for the defect-free model (Fig. 3b), but the existence of stacking faults can be detected by comparing the I_{101}/I_{102} and I_{110}/I_{102} ratios of the two curves. The differences in these ratios are due to a combined effect of an increase in \bar{H} (45 \AA vs. 68 \AA) and of the presence of stacking faults. Indeed, I_{110} has little dependence on \bar{H} whereas I_{101} has a strong dependence, and I_{102} is much more sensitive to the presence of stacking faults than the other peaks. The presence of stacking faults is much more apparent in the 6-component model inasmuch as it produces a substantial broadening and a decrease in intensity of the 102 reflection despite the relatively high \bar{H} value (68 \AA , Fig. 3c).

The Patrat et al. (1983) model

This model has three main features:

(a) With x and y fixed, vacant and occupied octahedra alternate along the c axis as Fe–Fe– \diamond – \diamond –Fe–Fe– \diamond – \diamond . . .

(b) The structure contains only two types of chains, denoted by numbers 0 and 3, or 1 and 2, along which vacant and occupied octahedra regularly alternate. These chains can be distributed irregularly over the hexagonal-lattice nodes of the ab plane with the limitation that, among each three chains passing through adjacent lattice nodes, two of them are the same type (Fig. 4b,c).

(c) In each pair of face-sharing occupied octahedra, one Fe atom is at the centre of the octahedron while the other is displaced from the centre by $\Delta = 0.6 \text{ \AA}$. The resulting Fe–Fe distance across faces is 2.88 \AA as in hematite (Fig. 4a).

The presence of chains of the types 0 and 3 distributed according to the pattern described above leads to three distinct Fe–Fe distances corresponding to pairs of edge-sharing (2.947 \AA), corner-sharing (3.39 \AA) and face-sharing (2.88 \AA) octahedra. The random

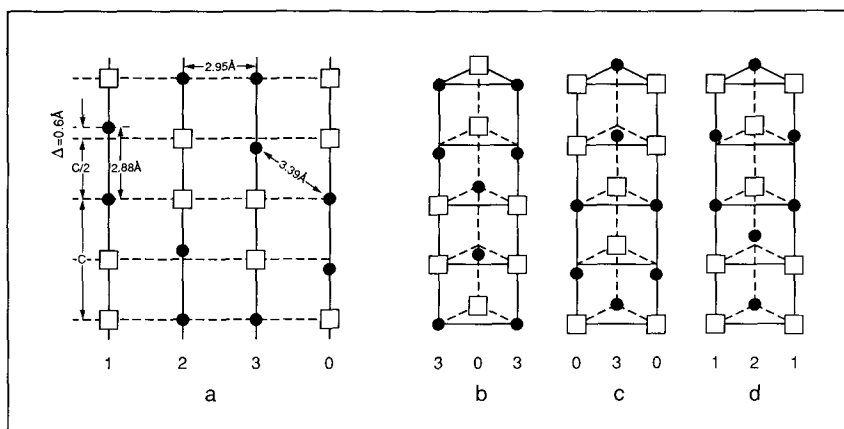


FIG. 4. Four types of chains differing in their Fe positions along the c axis (a) and three possible combinations of these in the δFeOOH structure (b,c,d). Open squares and filled circles represent vacancies and occupied Fe sites, respectively. Distances at 2.88, 2.95, and 3.39 \AA correspond to face-, edge-, and corner-sharing Fe–Fe distances. After Patrat *et al.* (1983).

distribution of these two different chains results in an average feroxyhite structure which is identical to that of Okamoto (1968) in all respects except the z -coordinates of Fe.

The XRD curve calculated for this model is presented in Fig. 2b. Irrespective of other parameters (CSD dimensions, contents of stacking faults etc . . .), this model is unacceptable because of a relatively strong 001 basal reflection at $d = 4.56 \text{ \AA}$ observed in the simulated XRD curve. This reflection is present because one of two Fe cations is displaced from the octahedral centre in face-sharing octahedral pairs; however, an asymmetric displacement of Fe atoms away from shared faces seems unjustified by crystal chemistry. This situation causes the two octahedra engaged in face-sharing to differ dramatically in cation-anion bond lengths: in one, all the six Fe-(O,OH) distances are 2.05 \AA long whereas, in the second, three Fe-(O,OH) distances are 2.35 \AA and the rest 1.75 \AA . This latter distance is abnormally short compared to those encountered in Fe (oxyhydr)oxides ($1.95 \text{ \AA} \times 3 + 2.09 \text{ \AA} \times 3$ in αFeOOH , Szytula *et al.*, 1968, and $1.95 \text{ \AA} \times 3 + 2.12 \text{ \AA} \times 3$ in $\alpha\text{Fe}_2\text{O}_3$, Blake *et al.*, 1966). In addition we have found that this model does not fit with EXAFS results. In αFeOOH and $\alpha\text{Fe}_2\text{O}_3$, the bimodal distribution of Fe-(O,OH) distances results in a wave-beating near 11 \AA^{-1} ($2k\Delta R = \pi$) observed on their Fourier filtered EXAFS spectra (Fig. 5 and Manceau & Drits, 1993). Examination of Fig. 5a and 5b shows that the Fe-(O,OH) contribution to EXAFS for feroxyhite is very similar to those for goethite and hematite, and displays the same beat-node pattern near 11 \AA^{-1} . This result proves that in feroxyhite, Fe-(O,OH) distances are similar to those in the (oxyhydr)oxide. The presence of 1.5(O,OH) at 1.75 \AA , 3(O,OH) at 2.05 \AA and 1.5(O,OH) at 2.35 \AA , conforming with the Patrat *et al.* model, would have resulted in a wave cancellation in the low k range since $2(5 \text{ \AA}^{-1})(2.35 \text{ \AA} - 2.05 \text{ \AA}) = 2(5 \text{ \AA}^{-1})(2.05 \text{ \AA} - 1.75 \text{ \AA}) \approx \pi$ (Fig. 5c).

The modified Patrat et al. (1983) model

The basal reflection at $d = 4.56 \text{ \AA}$ may be suppressed if it is assumed that local domains of two types coexist in a similar amount within the uniform anionic framework. One domain contains chains of types 0 and 3 (Fig. 4b,c) and the other contains chains of types 1 and 2 (Fig. 4d), with the same distribution rules as in the previous model. These two domains are equivalent as far as the local structure is concerned, and the basal reflection is suppressed by the lack of periodicity in Fe distribution as projected on to the c axis. In addition, it is more reasonable crystallochemically if, by analogy with hematite, Fe atoms were displaced by the same value of $\Delta = 0.3 \text{ \AA}$ in opposite directions away from shared faces (Fig. 6a). The shortest Fe-Fe distance would then remain 2.88 \AA but the two octahedra would now be equivalent with respect to Fe-(O,OH) bond lengths. With account taken of the two domains structure and of the symmetrical displacement of Fe, the positions and contents of atoms in the feroxyhite unit-cell will be those given in Table 2. There are two equivalent positions for each of Fe positions (z , \bar{z}). This symmetrical splitting of the z positions results from the mixing of the two domains, each of these having a unique z value for Fe atoms.

In Fig. 7a it can be seen that the 101 and 102 reflections in the XRD curve simulated for this model with $\bar{H} = 25 \text{ \AA}$ are practically equal in intensity. The XRD simulations would have given similar results if only one of every two nearest Fe cations was removed from its octahedral centre. Symmetric displacement of Fe atoms away from shared faces is in accord with EXAFS results and with crystal chemical considerations.

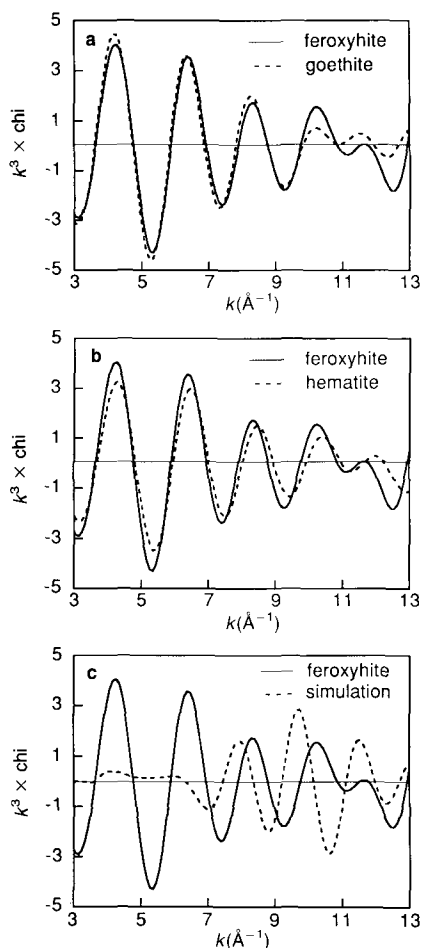


FIG. 5. Fourier filtered Fe-(O,OH) contributions to EXAFS. Comparison of experimental contributions for goethite and feroxyhite (a), and for hematite and feroxyhite (b). (c) Experimental contribution for feroxyhite compared to a simulated spectrum assuming 1.5 (O,OH) at 1.75 Å + 3.0 (O,OH) at 2.05 Å and 1.5 (O,OH) at 2.35 Å. Experimental details are given in Manceau & Drits (1993).

The modified Patrat et al. (1983) model containing stacking faults

The introduction of a six-component or a two-component model leads to diffraction effects similar to those reported for the Okamoto model (Fig. 3c,d) irrespective of the extent of stacking faults or \bar{H} values. In an XRD curve calculated for the 6-component model with $P_c = 0.15$ and $\bar{H} = 34$ Å (Fig. 7b), the 102 reflection drops and broadens compared to the defect-free model (Fig. 7a) despite an increase in \bar{H} value from 25 to 34 Å. The XRD curve plotted in Fig. 7c shows that compared with the defect-free model (Fig. 7a), the 2-component model increases the I_{101}/I_{102} ratio of peak heights. This ratio is >1 despite an increase of the average CSD thickness from 25 to 68 Å which tends to reverse this ratio as illustrated in Fig. 3a and 3b.

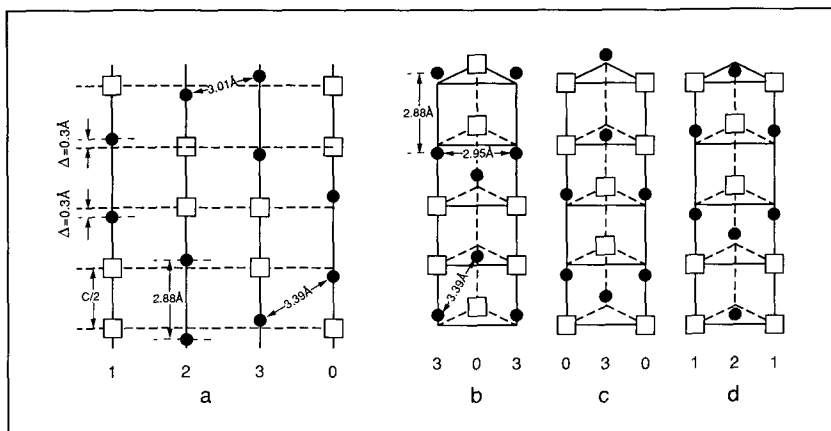


Fig. 6. Four types of Fe distribution along the c axis where Fe atoms are displaced from the centre of face-sharing octahedra in opposite directions by the same value $\Delta = 0.3 \text{ \AA}$ (a). On the right (b,c,d), three possible combinations of these chains. Open squares and filled circles represent vacancies and occupied Fe sites, respectively. Distances at 2.88, 2.95, and 3.39 \AA correspond to face-, edge-, and corner-sharing Fe-Fe distances.

The role of octahedral occupancies and "temperature" factors

The very small size of particles and the possible presence of admixed impurities has, to date, hampered determining whether the chemical composition of ferroxhyte conforms to the idealized formula FeOOH . Therefore, we have also simulated XRD curves for models having variable Fe occupancies. A decrease in Fe content by only 4–6% has been found to considerably increase the 101 reflection intensity with a preservation of intensity ratios for other reflections. Similar diffraction effects can be produced by different choices of "temperature" or Debye-Scherrer B factors for cations and anions. Specifically, quite similar XRD curves were observed for the two following models: (i) 42% occupancy of octahedra and $B = 2$ for all atoms; (ii) 50% octahedral occupancy but $B = 1$ and 3 for anions and cations, respectively. The XRD curve calculated for the former model is shown in Fig. 7d. The second model seems preferable because within a close-packed framework, the deviation of anions from their ideal sites is due mainly to thermal vibration. In contrast, Fe atoms may have a greater deviation from their average structural site because their actual position is influenced by both thermal vibration and static disorder.

TABLE 2. Atomic coordinates, site occupancy (P) and temperature factor (B) for ferroxhyte structural model.

Atom	x	y	z	P	$B(\text{\AA}^2)$
O in 6(i)	1/3	2/3	0.25	1	1
Fe in 2(c)	0	0	0.065	0.25	3
Fe in 2(c)	0	0	0.435	0.25	3

Space group $\text{P}\bar{3}\text{m1}$ (D_{3d}^3), $a = 2.947 \text{ \AA}$ and $c = 4.56 \text{ \AA}$.

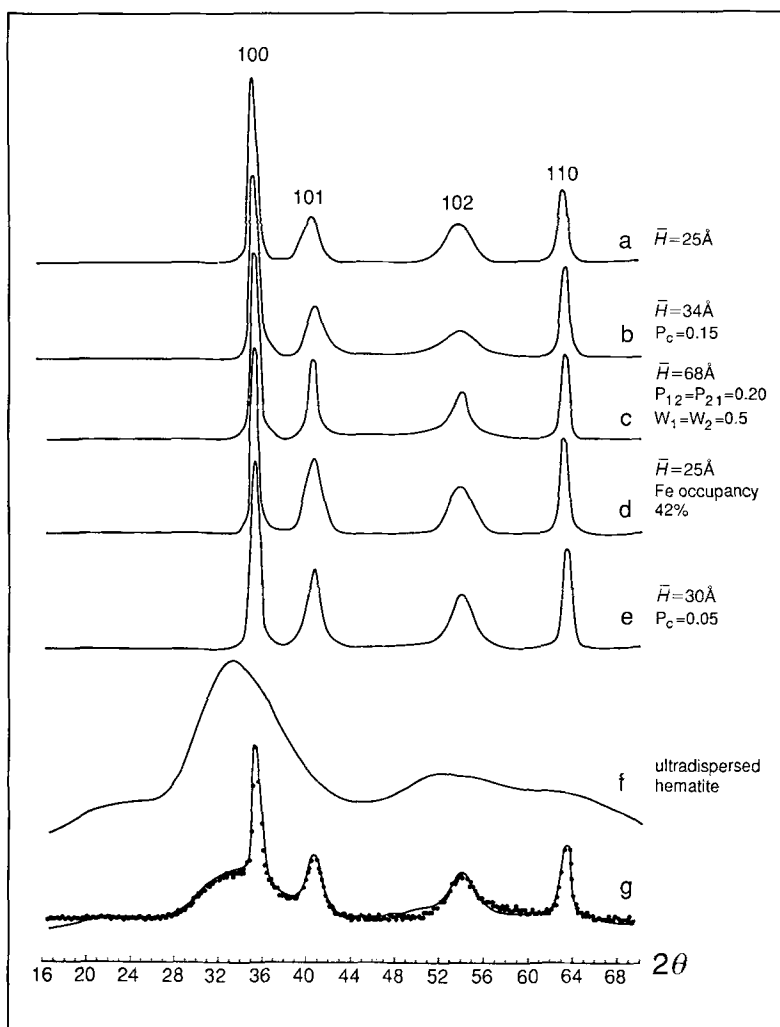


Fig. 7. XRD curves calculated for: (a) the modified Patrat *et al.* (1983) model containing no defects and disc-shaped CSD; 4, 5, 6 and 7 unit-cells are present with the same probability, $\bar{H} = 25 \text{ \AA}$; (b) the modified Patrat *et al.* (1983) model containing stacking faults, $W_i = 1/6$ ($i = 1, 2 \dots 6$), $P_c = 0.15$, $\bar{H} = 34 \text{ \AA}$; CSD with thickness equal to 5, 6 ... 10 unit-cells occur with equal probability; (c) the modified Patrat *et al.* (1983) model containing stacking faults, $W_1 = W_2$, $P_{12} = P_{21} = 0.20$, $\bar{H} = 68 \text{ \AA}$. CSD with thicknesses equal to 10, 11, 12 ... 20 unit-cells occur with equal probability; (d) the modified Patrat *et al.* (1983) model containing 42% Fe in each octahedron and $B = 1$ for all atoms; CSD with thicknesses equal to 4, 5, 6 and 7 unit-cells are present with the same probability, $\bar{H} = 25 \text{ \AA}$; (e) the modified Patrat *et al.* (1983) model containing 5% stacking faults and disc-shaped CSD, 110 \AA in diameter and 30 \AA in average thickness; CSD containing 3, 4, 5 ... 10 unit-cells occur with equal probability; (f) ultradispersed hematite powder sample containing cylinder-shape CSD 10 \AA in diameter; cylinders with height 9.15, 13.75 and 20.58 \AA occur with equal probability; (g) a mixture of feroxyhite and ultradispersed hematite in 9:1 volume ratio. Dots represents the experimental XRD data for the sample under study. Cu-K α radiation.

The choice of the feroxyhite model

Comparison of the experimental XRD curve with simulated ones has shown that the best agreement is observed with the modified Patrat *et al.* (1983) model containing 5% stacking faults, an octahedral Fe site occupancy of 50%, and with "temperature" factors equal to 1 and 3 for anions and cations, respectively (Fig. 7e,g). Nevertheless, these two curves still differ from each other because of the presence of a shoulder near the 100 reflection on the experimental XRD curve. This shoulder resembles one described elsewhere in ferrihydrite (Drits *et al.*, 1992) and, to the best of our knowledge, is present on all XRD patterns for δFeOOH samples yet published (Chukhrov *et al.*, 1973; Carlson & Schwertmann, 1980; Koch *et al.*, 1987). In their structural study of ferrihydrite, Drits *et al.* (1993) have shown that this shoulder arises from the presence of an ultradispersed hematite phase which is intimately associated with the ferrihydrite proper, and whose CSD can be treated as nuclei of the acicular hematite variety. By analogy, we have supposed that the sample under study is a mixture of feroxyhite microcrystals and ultradisperse hematite particles. Figure 7f shows an XRD curve simulated for a powder hematite sample containing cylindrical CSD, 10 Å in diameter. Cylinders 9.15, 13.75 and 20.58 Å thick were assumed to occur with equal probability. The XRD curve calculated for a model sample consisting of a mixture of feroxyhite and hematite in the 9:1 volume ratio corresponds well in reflection positions, relative intensities, and peak profiles, to the experimental curve (Fig. 7g).

DISCUSSION

The results obtained show that the basic structural features of feroxyhite, encompassing anion hexagonal close packing and Fe sites occupancy, agree in general with the Okamoto (1968) structural model. The introduction of 5% stacking faults and a minor portion of hematite impurities leaves the essence of the model unaffected, and these two minor modifications only promote better fitting of the experimental curve. The model chosen does not contradict the local structure suggested by Patrat *et al.* (1983) if we suppose the existence of two types of domains with the same volume probability and containing 0,3 and 1,2 types of chains. As noted above, XRD fails to distinguish between models containing 0,3 and 1,2 chains but differing in mutual arrangement of Fe atoms in face-sharing octahedra (compare Figs. 4 and 6). Although these two models have the same set of Fe–Fe distances (2.88, 2.95 and 3.39 Å), they differ in their Fe–(O,OH) distances. The presence of vacant and occupied sites having different sizes and relative distributions, however, makes it impossible to determine precisely Fe–(O,OH) bond lengths by diffraction methods. The unit-cell parameters permit us to estimate only the statistically weighted distance between the centres and corners of vacant and occupied octahedra, equal to 2.048 Å. On a crystal chemical basis, the modified Patrat *et al.* model where both face-sharing octahedra are equivalent with respect to bond-length distribution seems more plausible than the original model. This finding is confirmed by the EXAFS analysis since the distribution of distances in Fe octahedra was found to be quite identical to those in αFeOOH and $\alpha\text{Fe}_2\text{O}_3$.

The EXAFS analysis of Fe–Fe pairs indicates that, on average, each octahedron is surrounded by 1.2 ± 0.5 Fe at 2.91 Å, 1.8 ± 0.5 Fe at 3.04 Å and 2.7 ± 0.5 Fe at 3.41 Å (Manceau & Drits, 1993). The shortest and longest distances agree with our structural model since 2.91 Å could be considered as a mean-weighted value of 2.88 and 2.95 Å (Figs. 4a, 6a), whereas 3.41 Å is close to 3.39 Å. But to explain the origin of the 3.04 Å

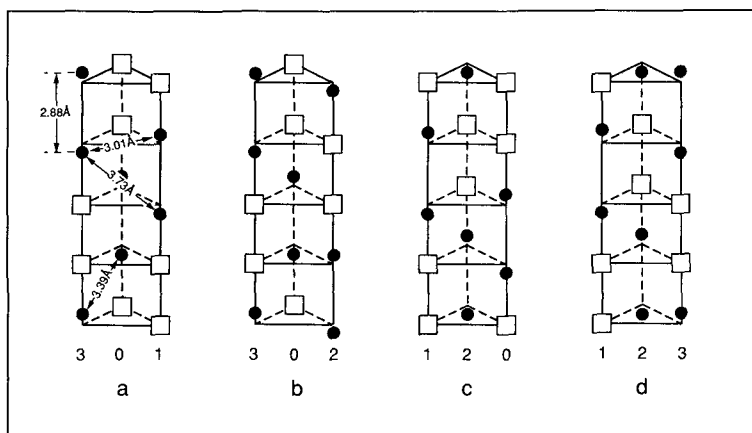


FIG. 8. Possible local structure for feroxyhite consisting of trigonal prisms formed by three different Fe chains. Open squares and filled circles represent vacancies and Fe occupied sites, respectively. Distances at 2.88, 3.01, and 3.39–3.73 Å correspond to face-, edge-, and corner-sharing Fe–Fe distances.

Fe–Fe distance, one has to assume the presence of local structures somewhat different from those considered up to now. Let us, for instance, suppose the presence of chains forming, in the ab plane, triangles of the type 3-0-1, 3-0-2, 1-2-0, and 1-2-3 in addition to Fe–Fe distances of 2.88 and 3.39 Å; new distances of 3.01 and 3.73 Å thus appear while Fe–Fe pairs at 2.95 Å are now absent (Fig. 8). One of these new distances is close to the 3.04 Å EXAFS distance while the existence of the second one at ≈ 3.7 – 3.8 Å was suspected in the EXAFS analysis (Manceau & Drits, 1993). Although combinations of three distinct types of chains (3-0-1, 3-0-2 etc. . .) are not allowed by the Patrat *et al.* (1983) model, their possible existence cannot be altogether discarded. Quite possibly, the new set of Fe–Fe and Fe– \diamond distances and their occurrence probabilities may lead to a Fourier-transform of the diffuse scattering intensity close to that obtained by these authors. In addition, combinations of three chain types to form trigonal prisms do not exclude the possible coexistence of similar combinations of two chain types, i.e. of a domain structure. In this case, δFeOOH would have four nearest Fe–Fe distances equal to 2.88, 2.95, 3.01 and 3.39 Å. A more reliable determination of the cation distribution in δFeOOH is needed to ensure a less ambiguous choice among the possible local structures described.

ACKNOWLEDGMENTS

We thank J. Pannetier and J. Walker for their constructive reviews of the manuscript and helpful suggestions.

REFERENCES

- BERNAL J.D., DASGUPTA D.R. & MACKAY A.L. (1959) The oxides and hydroxides of iron and their structural inter-relationships. *Clay Miner. Bull.* **4**, 15–30.
- BLAKE R.L., HESSEVICK R.E., ZOLTAI T. & FINGER L. (1966) Refinement of the hematite structure. *Am. Miner.* **51**, 123–129.
- CARLSON L. & SCHWERTMANN U. (1980) Natural occurrence of feroxyhite (δFeOOH). *Clays Clay Miner.* **28**, 272–280.

- CHUKHROV F.V., ZVYAGIN B.B., ERMILOVA L.P. & GORSHKOV A.I. (1973) New data on iron oxides in the weathering zone. *Proc. Int. Clay Conf. Madrid*, 333–341.
- CHUKHROV F.V., ZVYAGIN B.B., GORSHKOV A.I., YERMILOVA L.P., KOROVUSHKIN V.V., RUDNITSKAYA Y.S. & YAKUBOVSKAYA N.YU. (1976) Feroksigit-novaya modifikatsiya FeOOH (Feroxyhite, a new modification of FeOOH). *AN SSSR Izvestiya, ser. Geol.* 5–24. (Transl. *Int. Geol. Rev.* **19**, 873–890).
- DASGUPTA D.R. (1961) Topotactic transformation in iron oxides and hydroxides. *Indian J. Phys.* **35**, 401–419.
- DRITS V.A. & TCHOUBAR C. (1990) *X-ray Diffraction of Disordered Lamellar Structures. Theory and Application to Microdivided Silicates and Carbons*. Springer-Verlag, Berlin.
- DRITS V.A., SAKHAROV B.A., SALYN A.L. & MANCEAU A. (1992) Structural model for ferrihydrite. *Clay Miner.* **28**, 185–207.
- FEITKNECHT W., HANI H. & DVORAK V. (1969) The mechanism of the transformation of δ -FeOOH to α -Fe₂O₃. Pp. 237–245 in: *Reactivity of Solids*. (J.W. Mitchell, R.C. De Vries, R.W. Roberts & P. Cannon, editors). Wiley, New York.
- FRANCOMBE M.H. & ROOKSBY H.P. (1959) Structure transformations effected by the dehydration of diaspore, goethite and delta ferric oxide. *Clay Miner. Bull.* **4**, 1–14.
- GLEMSER O. & GWINNER E. (1939) Uber eine neue ferromagnetische Modifikation des Eisen(III)-Oxydes. *Z. Anorg. Chem.* **240**, 163–171.
- KOCH C.J.W., BORGGAAARD O.K., MADSEN M.B. & MORUP S. (1987) Magnetic properties of synthetic feroxyhite (δ -FeOOH). *Proc. Int. Clay Conf. Denver*, 212–220.
- MANCEAU A. & DRITS V.A. (1992) Local structure of ferrihydrite and feroxyhite by EXAFS spectroscopy. *Clay Miner.* **28**, 165–184.
- MISAWA T., SUETAKA W. & SHIMODAIRA S. (1970) Formation of iron oxide and oxyhydroxides and aqueous solutions and their physical properties. *Zairyo* **19**, 537–542.
- OKAMOTO S. (1968) Structure of δ -FeOOH. *J. Am. Ceram. Soc.* **51**, 594–599.
- PATRAT G., DE BERGEVIN F., PERNET M. & JOUBERT J.C. (1983) Structure locale de δ -FeOOH. *Acta Cryst.* **B39**, 165–170.
- PERNET M., OBRADORS X., FONTCUBERTA J., JOUBERT J.C. & TEJADA J. (1984) Magnetic structure and supermagnetic properties of δ -FeOOH. *IEEE Trans. Magnetics* **20**, 1524–1526.
- PLANÇON A. (1981) Diffraction by layer structures containing different kinds of layers and stacking faults. *J. Appl. Cryst.* **14**, 300–304.
- POVITSKII V.A., MAKAROV E.F., MURAHKO N.V. & SALUGIN A.N. (1976) Mössbauer study of superparamagnetic δ -FeOOH and its transformation into α -Fe₂O₃. *Phys. Status Solidi* **A33**, 783–787.
- SAKHAROV B.A., NAUMOV A.S. & DRITS V.A. (1982a) X-ray diffraction by mixed-layer structures with random distribution of stacking faults. *Dokl. Akad. Nauk. SSSR* **265**, 339–343 (in Russian).
- SAKHAROV B.A., NAUMOV A.S. & DRITS V.A. (1982b) X-ray intensities scattered by layer defective structures with short range ordering factors $S \geq 1$ and $G \geq 1$. *Dokl. Akad. Nauk. SSSR* **265**, 871–874 (in Russian).
- SZYTLA A., BUREWICZ A., DIMITRIJEVIC Z., KRASNICKI S., RZANY H., TODOROVIC J., WANIC A. & WOLSKI W. (1968) Neutron diffraction studies of α -FeOOH. *Phys. Status Solidi* **26**, 429–434.